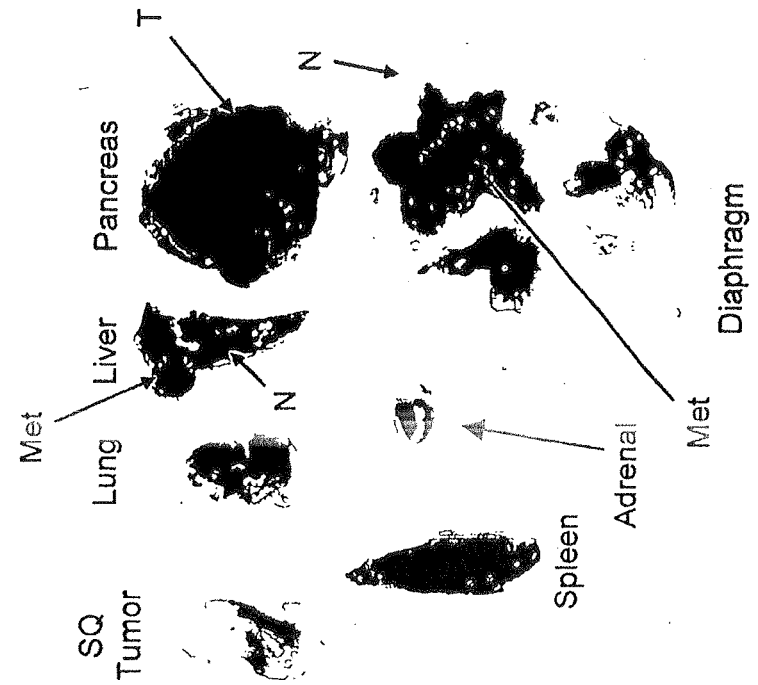

T
N
Pancreas
Liver
Met
N
Lung
SQ
Tumor
Spleen
Adrenal
Met
Diaphragm

FIG.1B

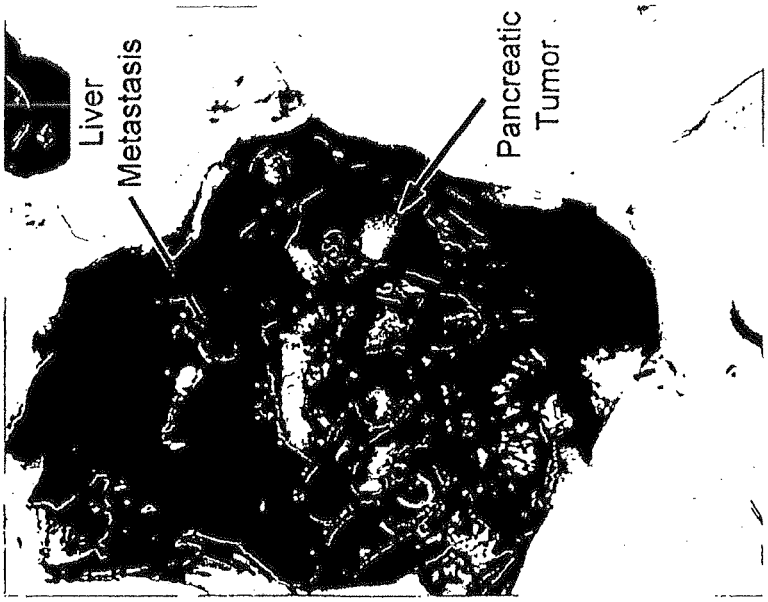

Liver
Metastasis
Pancreatic
Tumor

FIG.1A

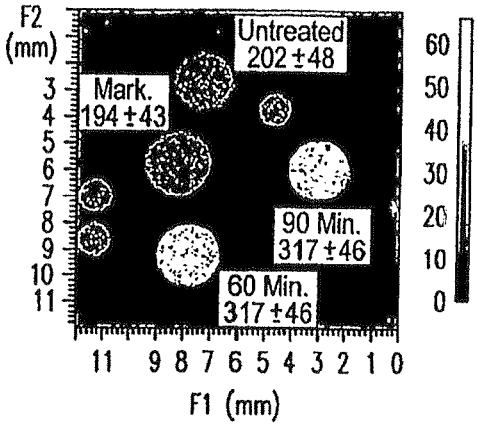


FIG.2A

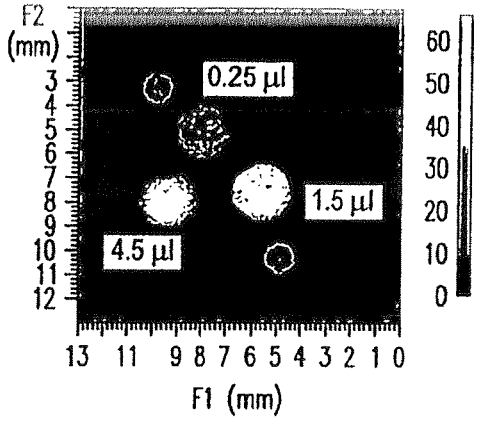


FIG.2B

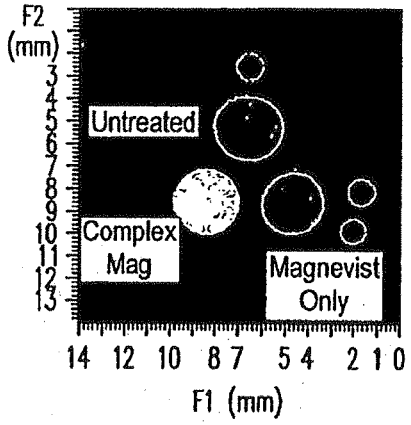


FIG.2C

Baseline

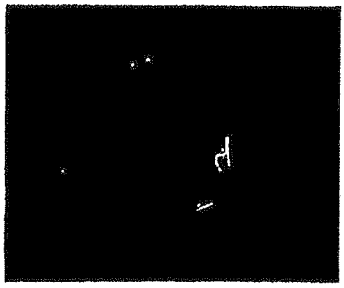


FIG.3A

Free Magnevist

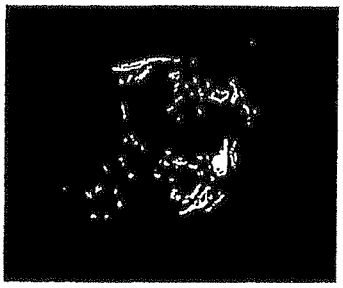


FIG.3D

Nanocomplex-Mag

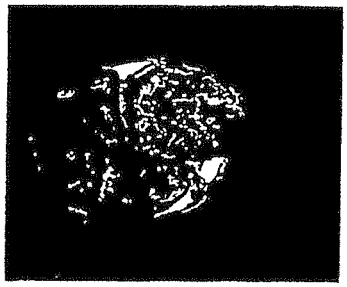


FIG.3G

Baseline



FIG.3B

Free Magnevist



FIG.3E

Nanocomplex-Mag

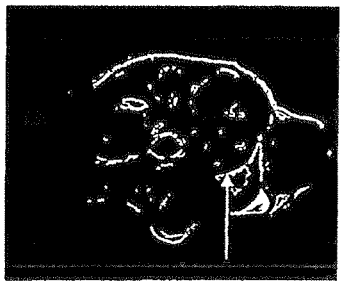


FIG.3H

Baseline

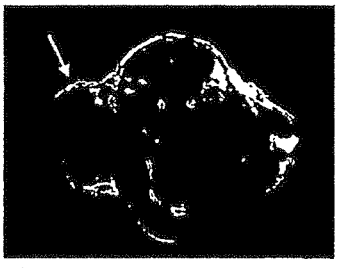


FIG.3C

Free Magnevist

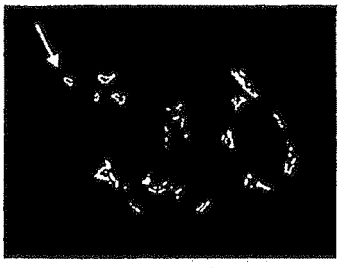


FIG.3F

Nanocomplex-Mag

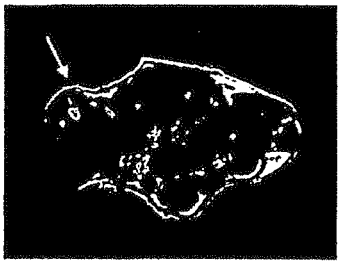


FIG.3I

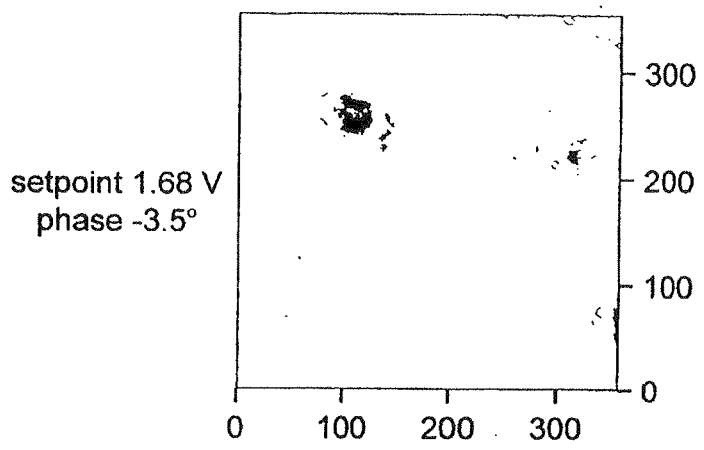


FIG.4A

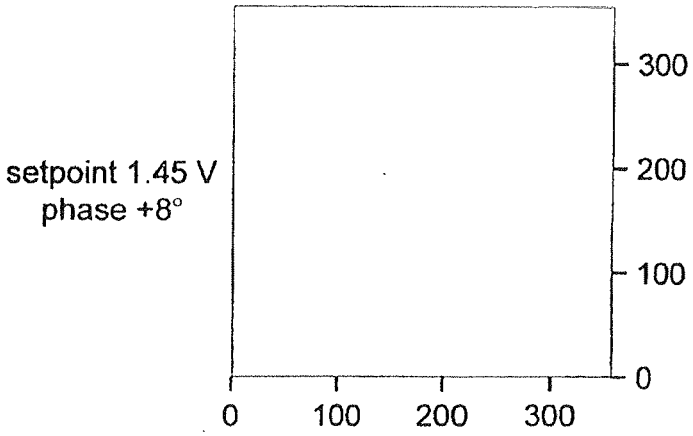


FIG.4B

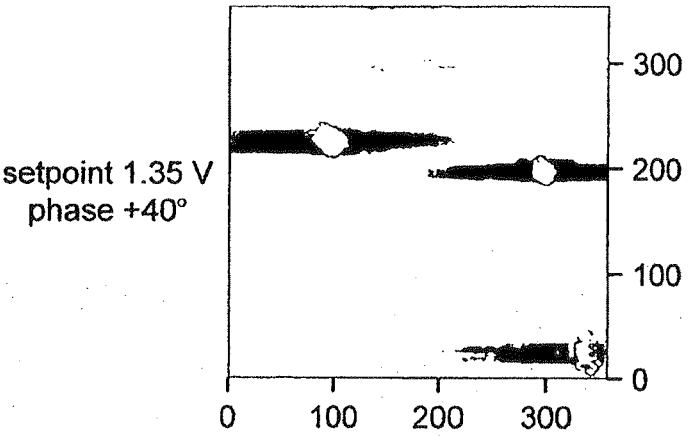


FIG.4C

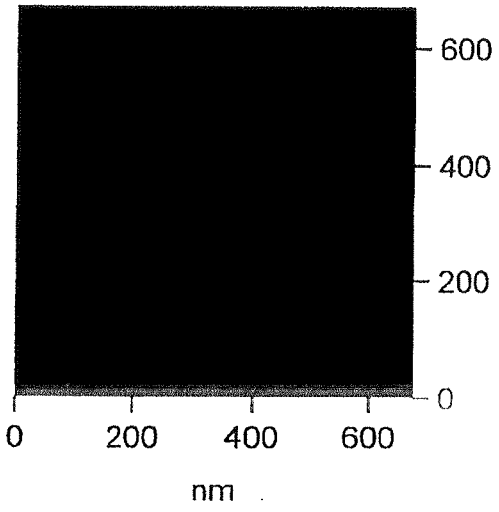


FIG.5A

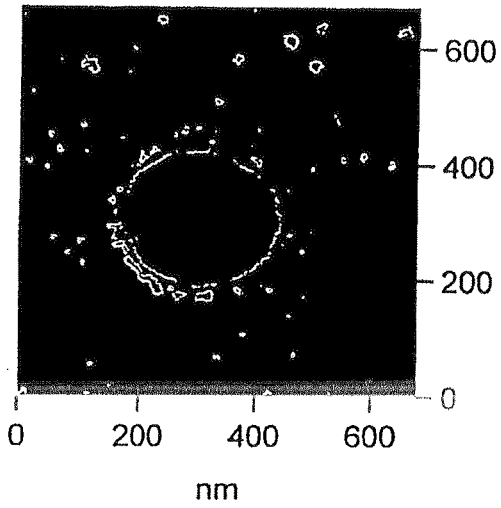


FIG.5B

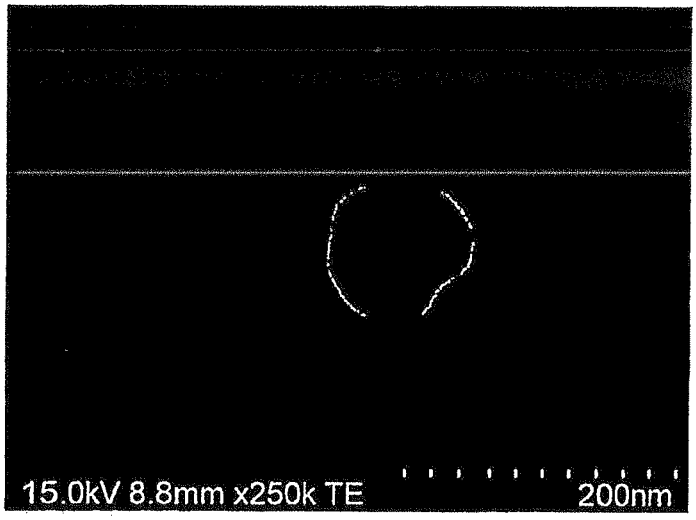


FIG.5C

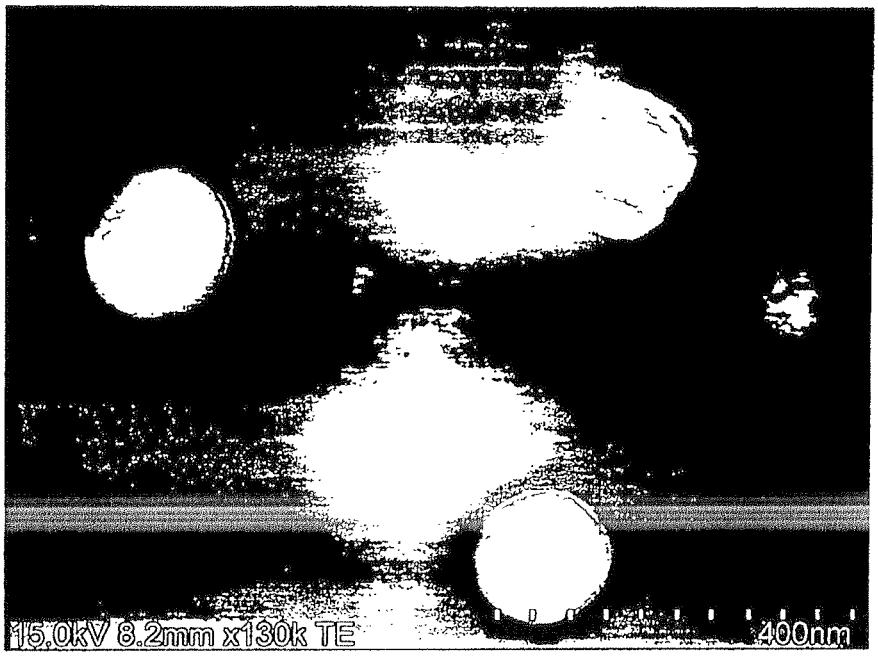


FIG.6A

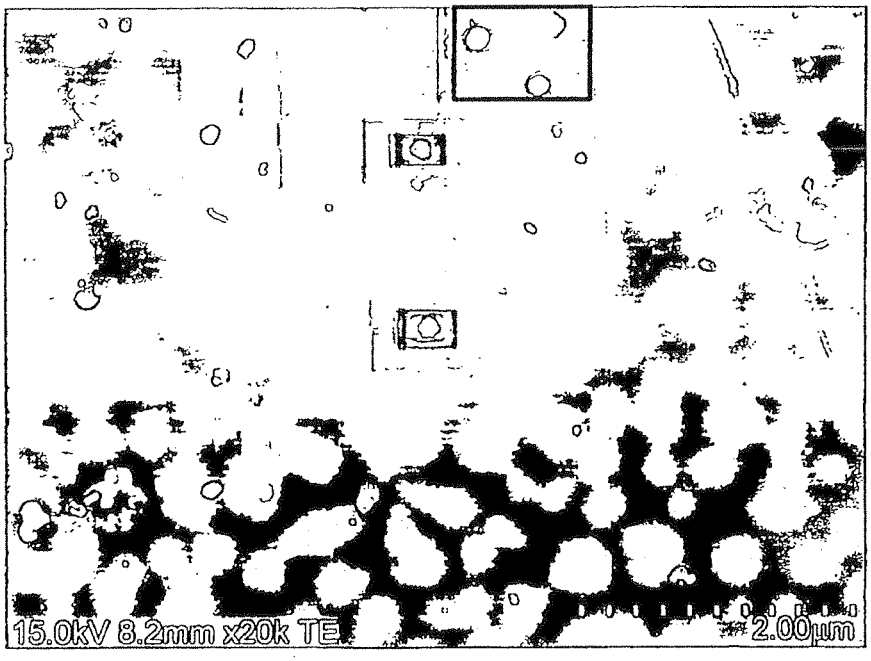


FIG.6B

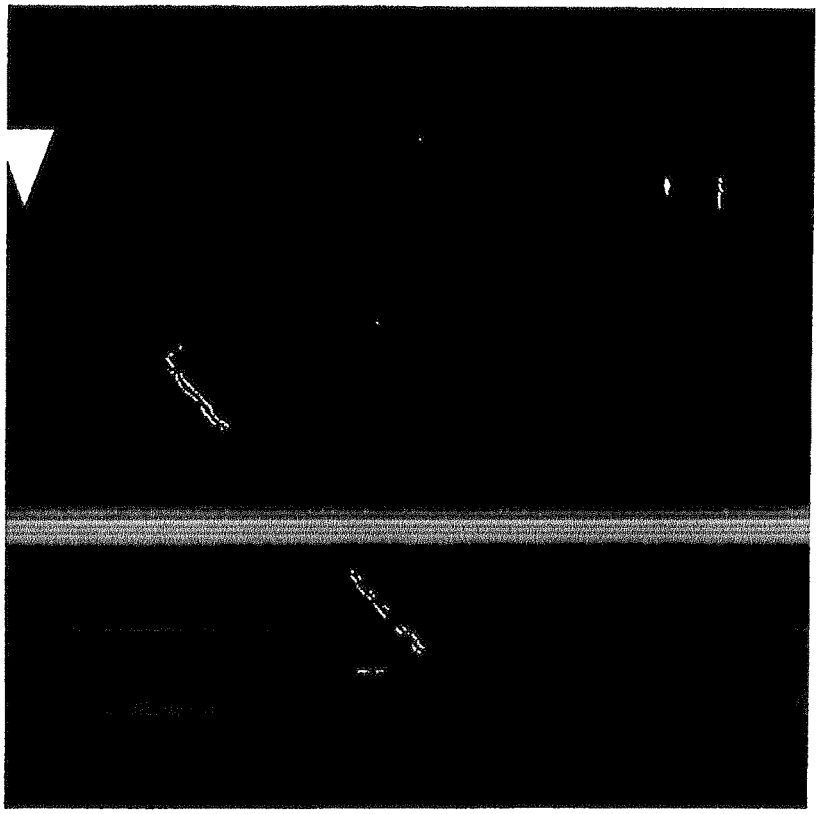


FIG. 7A

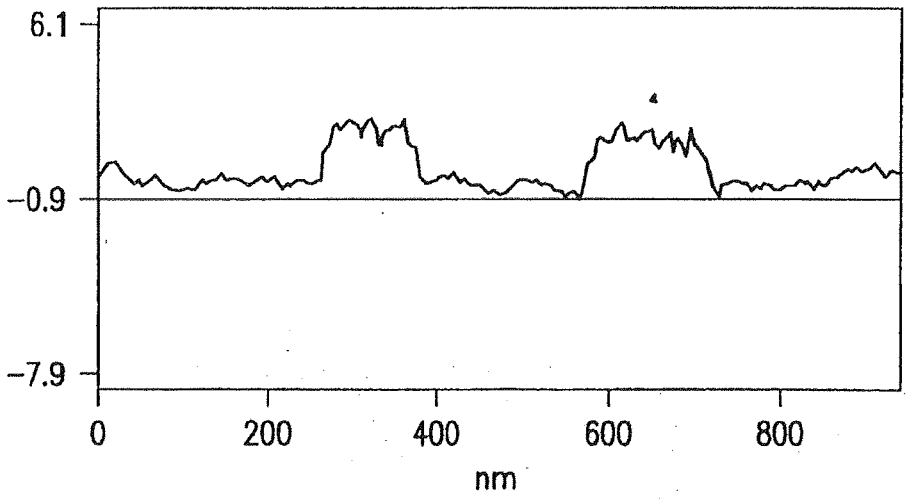


FIG. 7B

MR Imaging of DU145 Tumors by Ligand-Liposome Complexes

Baseline

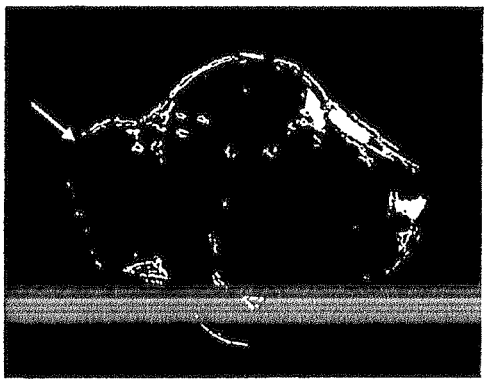


FIG.8A

Free Mag

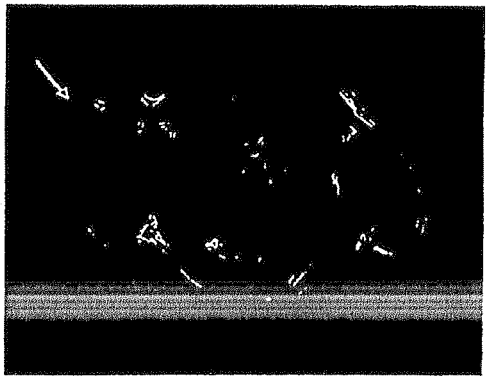


FIG.8B

scLip-Mag

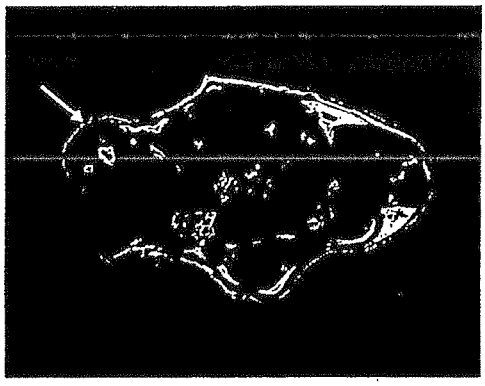


FIG.8C

scLip-HK-Mag

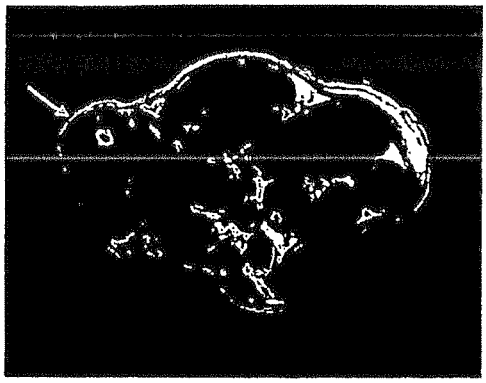


FIG.8D

Improved MR Imaging of MDA-MB-435 Tumors by 3rd Generation Ligand-Liposome Complex

Baseline

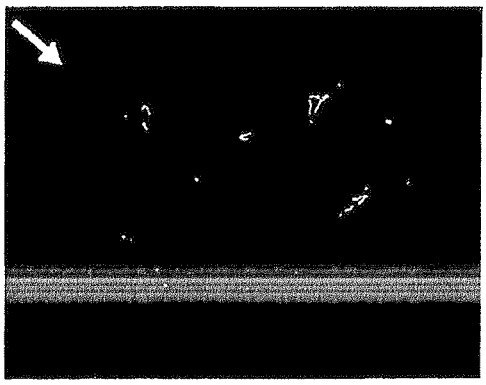


FIG.8E

Free Mag

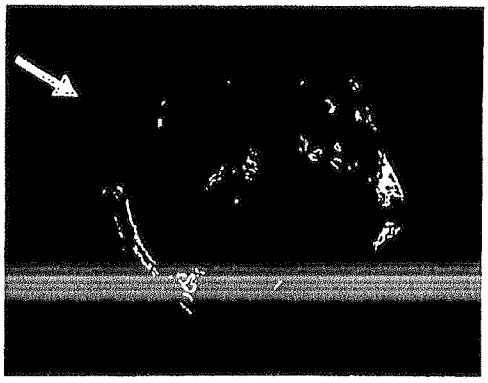


FIG.8F

scLip-Mag

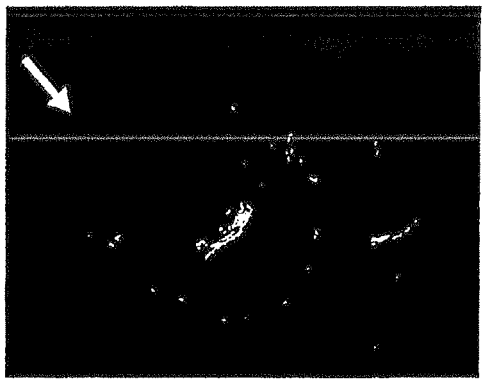


FIG.8G

scLip-HK-Mag

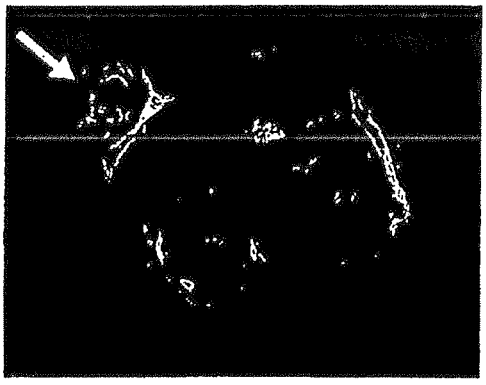


FIG.8H

Improved MRI Imaging of Pancreatic Tumor and Metastatic Lesions
Using 3rd Generation Nanocomplex Including the HK Peptide

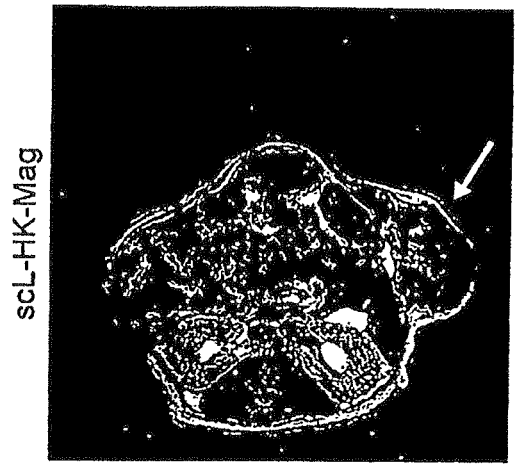


FIG.9C

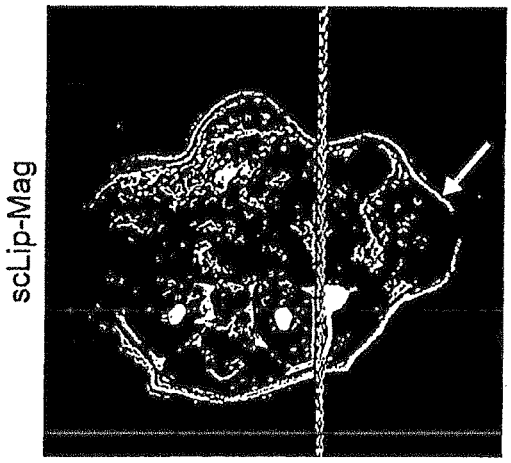


FIG.9B

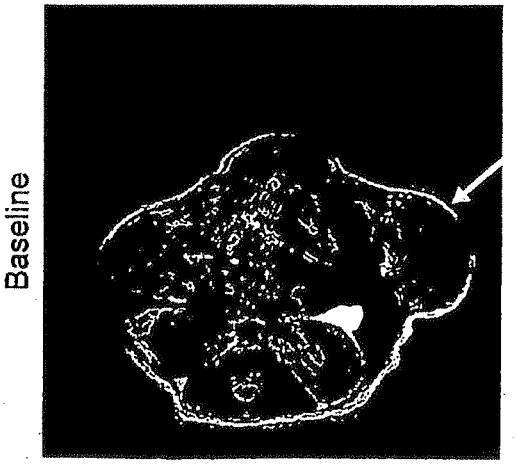


FIG.9A

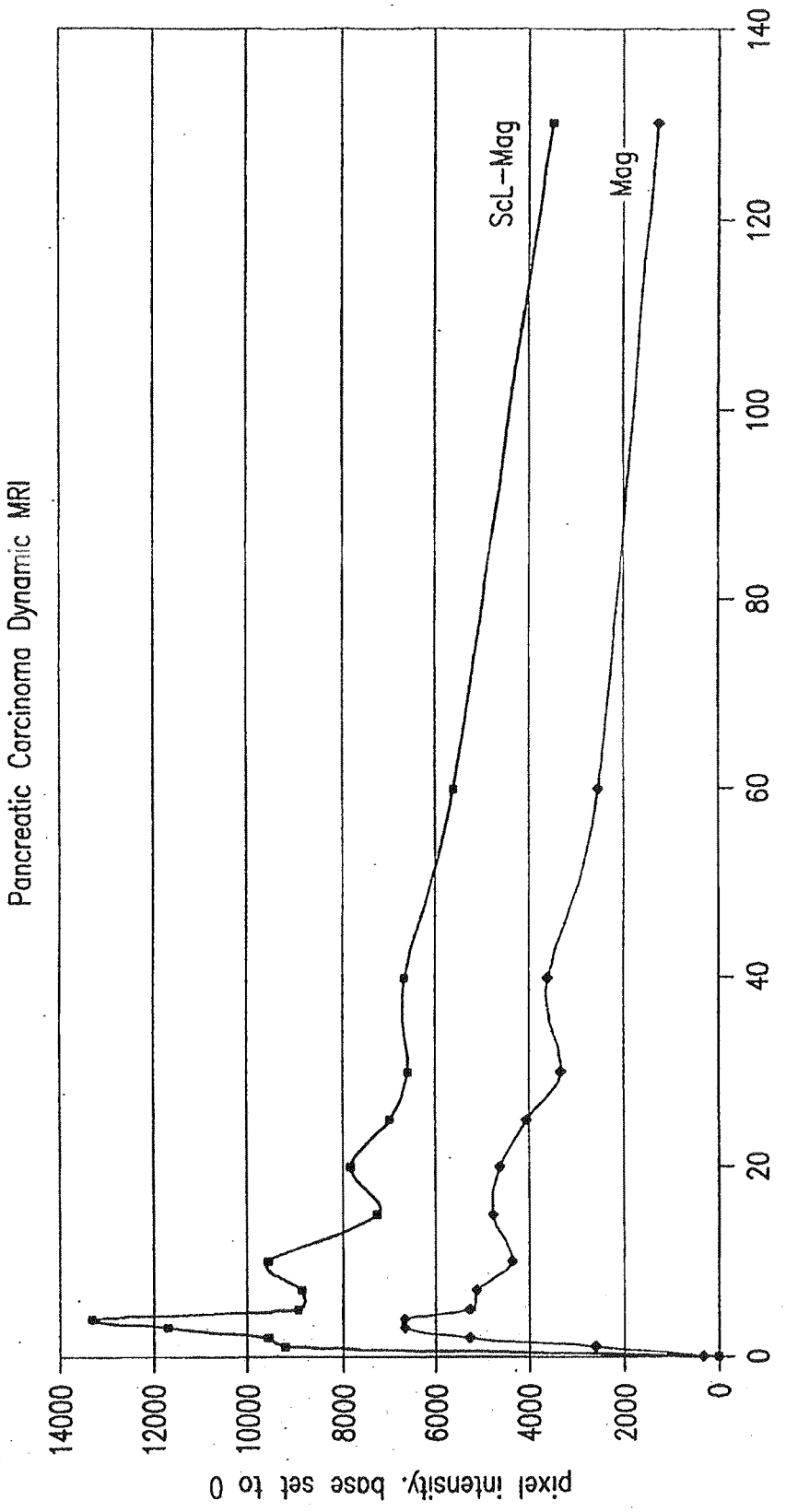
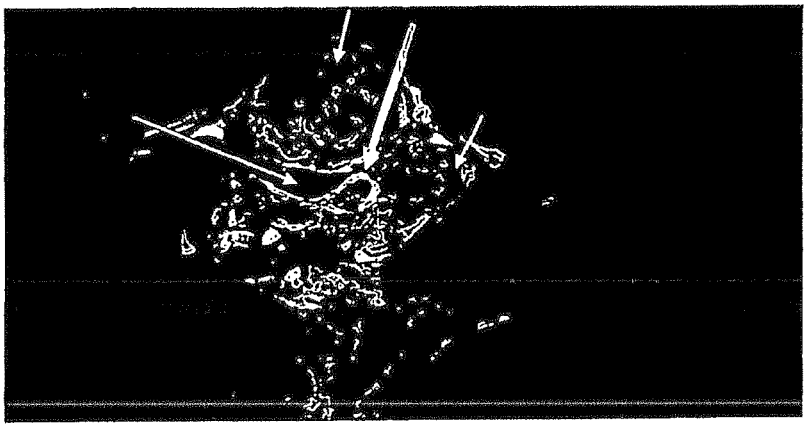

Pancreatic Carcinoma Dynamic MRI
pixel intensity, base set to 0
14000
12000
10000
8000
6000
4000
2000
0
0
20
40
60
80
100
120
140
time in minutes
ScL-Mag
Mag

FIG.10

MR Imaging of Pancreatic cancer metastasis by systematically delivered Nanocomplex gad-d



FIG.11C



Complex

FIG.11B



Baseline

FIG.11A

Greater Enhancement of Metastases on MRI Images with Complex vs Gad-d p<0.04 for six matched nodules
(25 days post-inoculation)

PI = Pixel intensity



Base (PI 5413)

FIG.12A

Complex (PI 10137)

FIG.12B



Base (PI 6313)

FIG.12C

Gad-d (PI)

FIG.12D

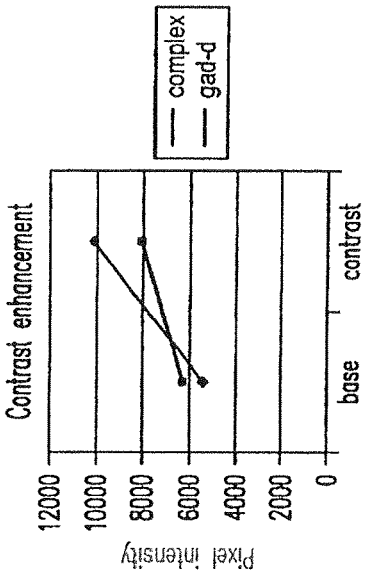


FIG.12E



FIG. 13A

FIG. 13B

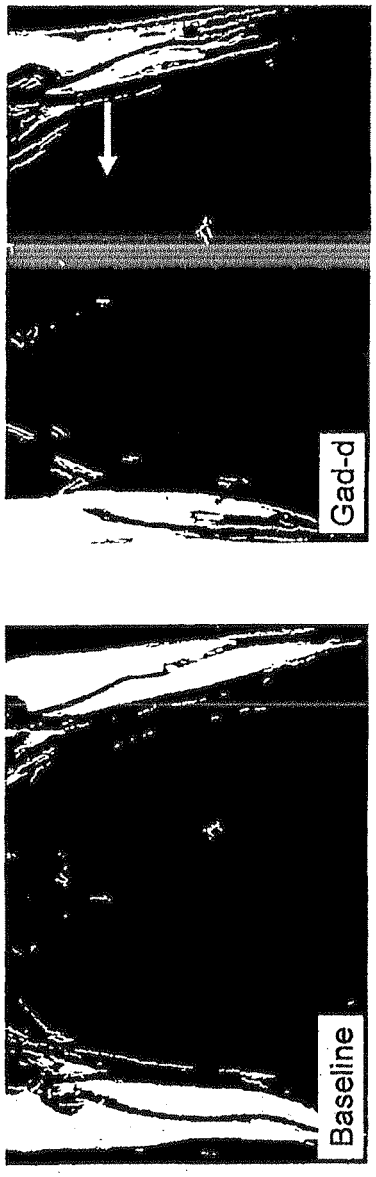


FIG. 13C

FIG. 13D

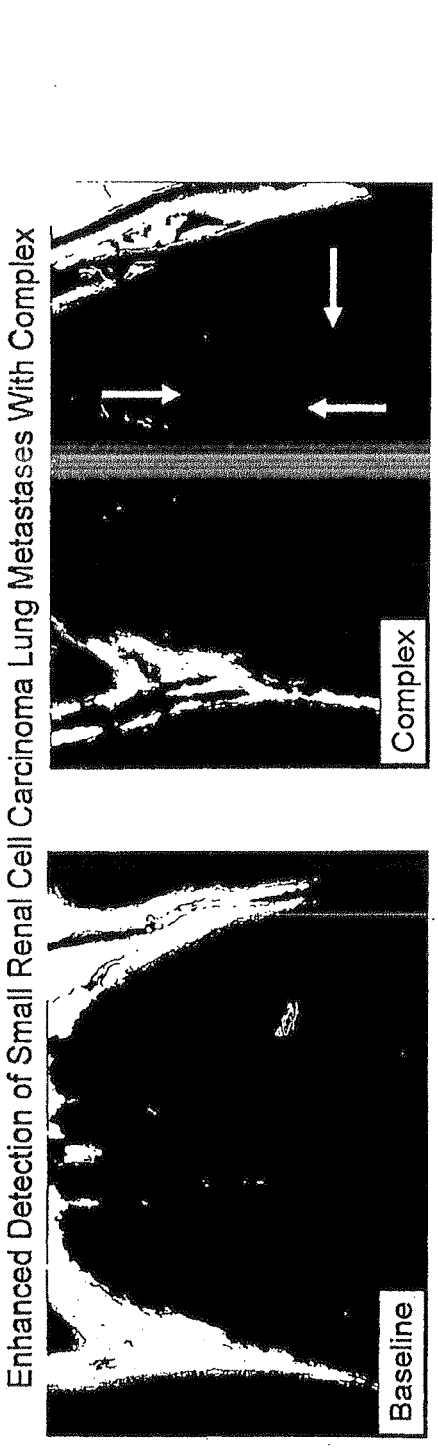


FIG. 14A

FIG. 14B

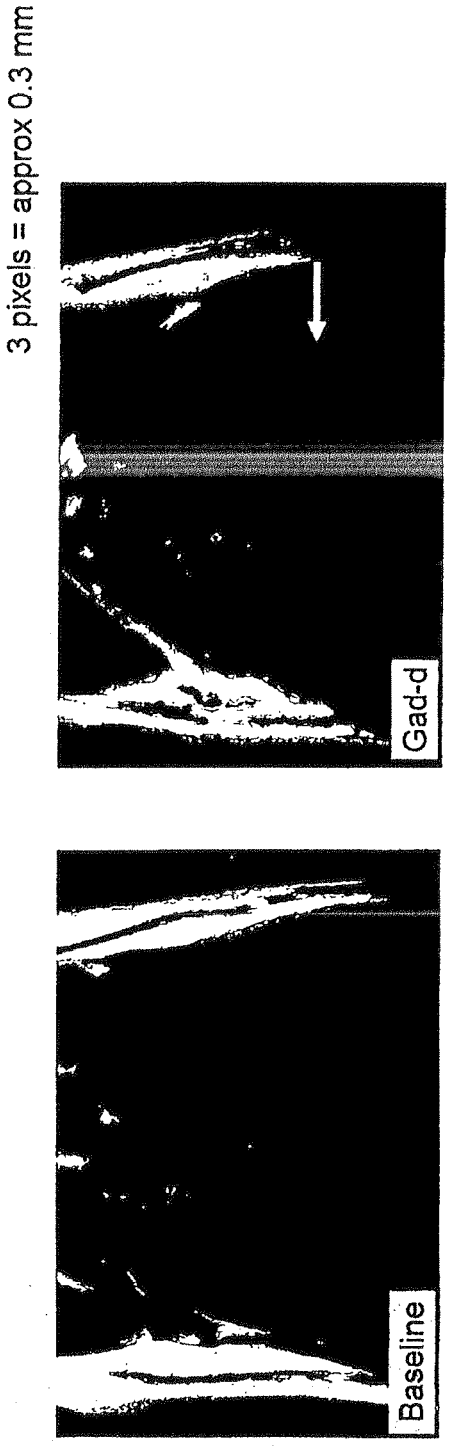


FIG. 14C

FIG. 14D

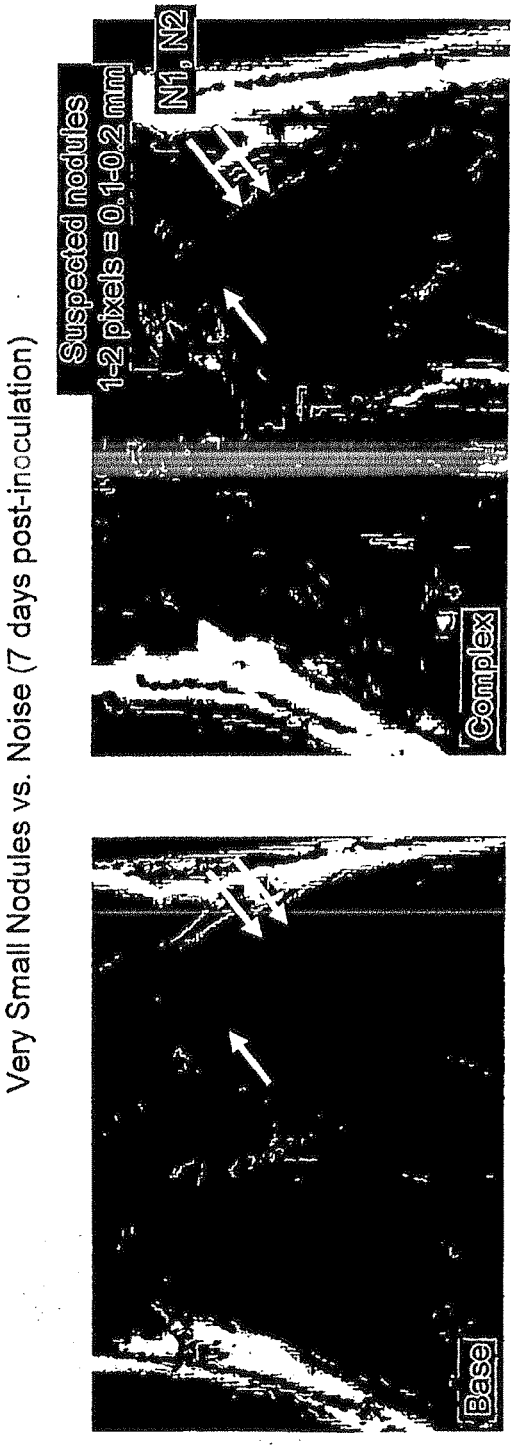


FIG.15A

		Mean	sd	max
Nodule 1	Base	566	278	1588
	comp	981	515	2542
Nodule 2	Base	591	299	1589
	comp	665	339	2274

The max value of Nodule 2 with complex is ≥2 SD above max base value

FIG.15B



FIG.16

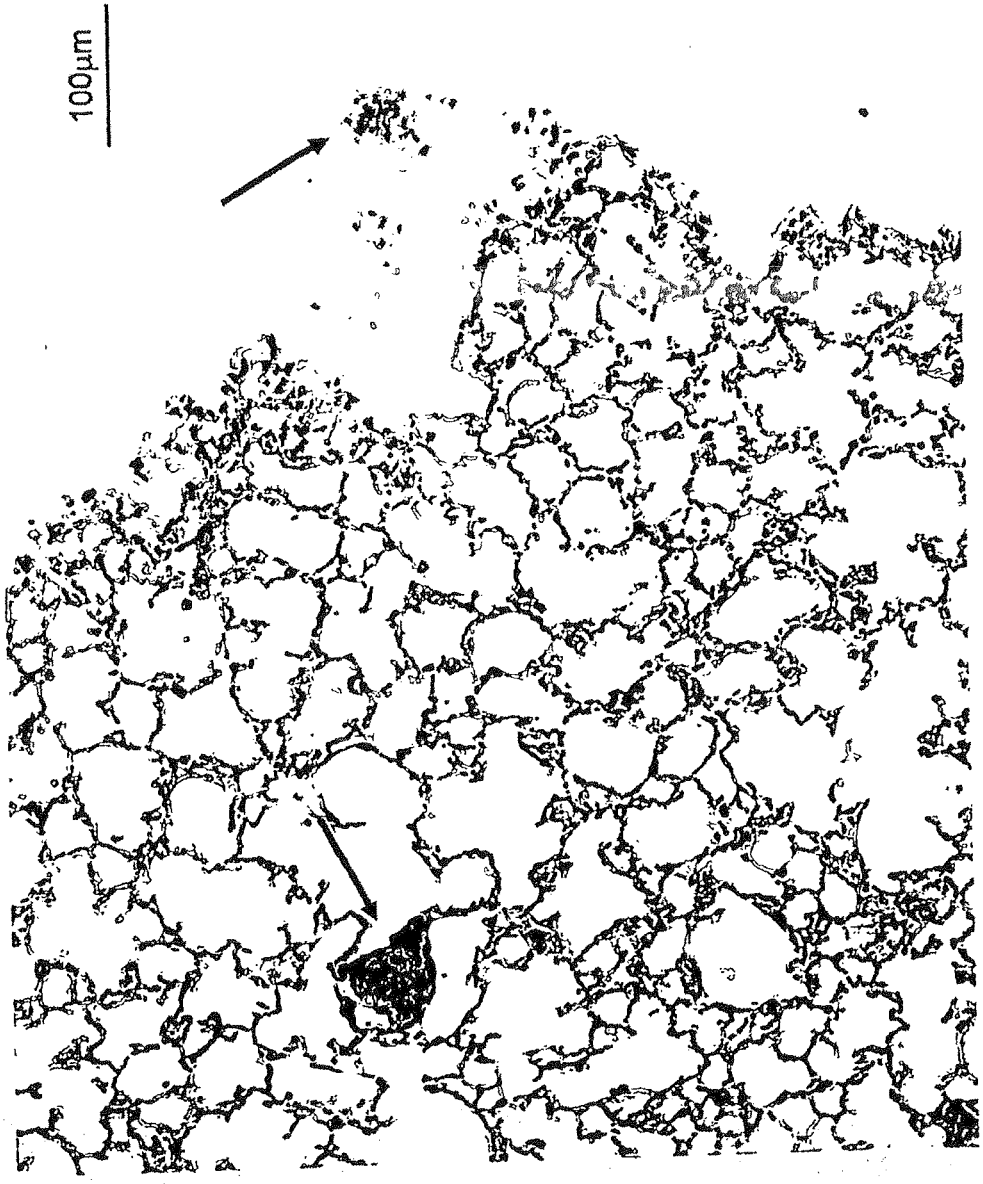
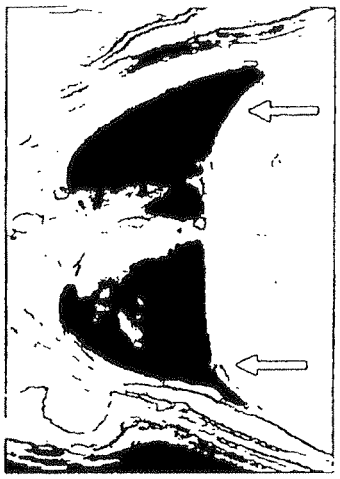


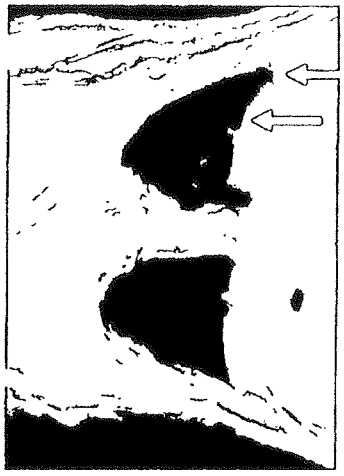
FIG.17

Renal Cell Carcinoma Sub pleural metastases
Two slices (8 days post-inoculation)



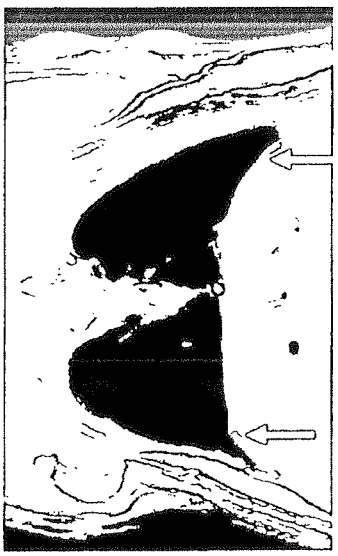
Complex at 2 hr

FIG.18C



Complex at 2 hr

FIG.18F



Complex at 1 hr

FIG.18B



Complex at 1 hr

FIG.18E



Base

FIG.18A



Base

FIG.18D

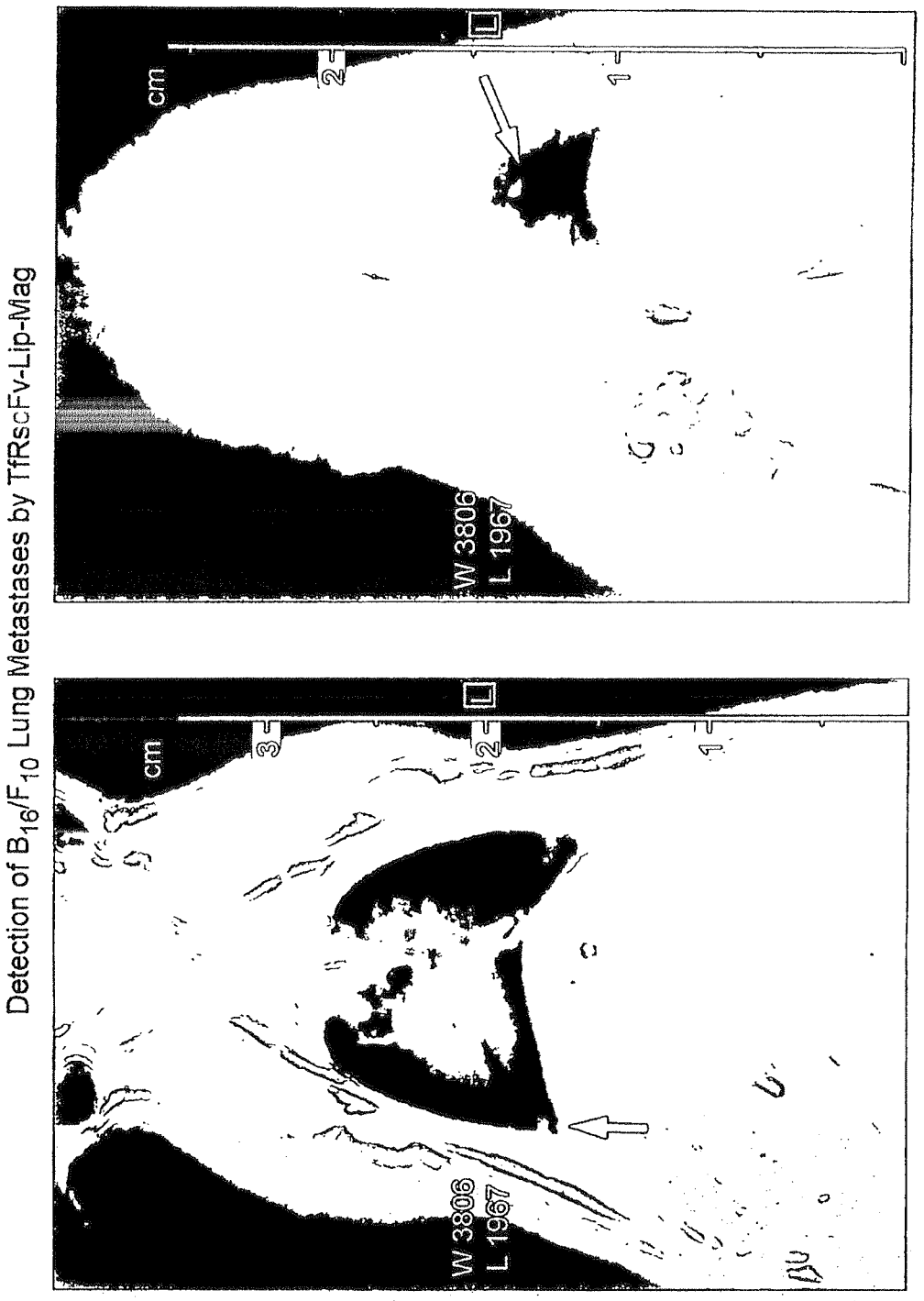


FIG. 19A

FIG. 19B

SEQUENCE LISTING

<110> Georgetown University
Chang, Esther H.
Pirollo, Kathleen F.

<120> Tumor-Targeted Nanodelivery Systems to Improve Early MRI Detection of Cancer

<130> 2474.006PC01

<150> US 60/728,303
<151> 2005-10-20

<160> 1

<170> PatentIn version 3.3

<210> 1
<211> 31
<212> PRT
<213> Artificial Sequence

<220>
<223> Chemically synthesized - HoKC

<400> 1

Lys Lys His Lys Lys Lys Lys His Lys Lys Lys Lys His Lys Lys Lys
1 5 10 15

Lys His Lys Lys Lys Lys His Lys Lys Lys Lys His Lys Lys Cys
20 25 30